Medicine®

OPEN

Value of intravoxel incoherent motion and dynamic contrast-enhanced MRI for predicting the early and short-term responses to chemoradiotherapy in nasopharyngeal carcinoma

Jing Hou, MM[a,b], Xiaoping Yu, MD[b,c,*], Yin Hu, MM[c], Feiping Li, MM[b], Wang Xiang, MM[b], Lanlan Wang, MM[b], Hui Wang, MD[c], Qiang Lu, MB[b], Zhongping Zhang, MD[d], Wenbin Zeng, PhD[a,*]

Abstract

The aim of the study was to investigate the value of intravoxel incoherent motion diffusion-weighted magnetic resonance imaging (IVIM-DWI) and dynamic contrast-enhanced magnetic resonance imaging (DCE-MRI) in predicting the early and short-term responses to chemoradiotherapy (CRT) in patients with nasopharyngeal carcinoma (NPC).

Forty-three NPC patients underwent IVIM-DWI and DCE-MRI at baseline (pretreatment) and after the first cycle of induction chemotherapy (posttreatment). Based on whether locoregional lesions were identified, patients were divided into the residual and nonresidual groups at the end of CRT and into the good-responder and poor-responder groups 6 months after the end of CRT. The pretreatment and posttreatment IVIM-DWI parameters (ADC, D, $D*$, and f) and DCE-MRI parameters (K^{trans}, K_{ep}, and V_e) values and their percentage changes ($\Delta\%$) were compared between the residual and nonresidual groups and between the good-responder and poor-responder groups.

None of perfusion-related parametric values derived from either DCE-MRI or IVIM-DWI showed significant differences either between the residual and nonresidual groups or between the good-responder and poor-responder groups. The nonresidual group exhibited lower pre-ADC, lower pre-D, and higher $\Delta\%D$ values than did the residual group (all $P < 0.05$). The good-responder group had lower pre-D and pre-ADC values than did the poor-responder group (both $P < 0.05$). Based on receiver operating characteristic (ROC) curve analysis, pre-D had the highest area under the curve in predicting both the early and short-term responses to CRT for NPC patients (0.817 and 0.854, respectively).

IVIM-DWI is more valuable than DCE-MRI in predicting the early and short-term response to CRT for NPC, and furthermore diffusion-related IVIM-DWI parameters (pre-ADC, pre-D, and $\Delta\%D$) are more powerful than perfusion-related parameters derived from both IVIM-DWI and DCE-MRI.

Abbreviations: ADC = apparent diffusion coefficient, CRT = chemoradiotherapy, DCE-MRI = dynamic contrast-enhanced magnetic resonance imaging, DWI = diffusion-weighted imaging, IC = induction chemotherapy, IVIM-DWI = intravoxel incoherent motion diffusion-weighted imaging, MRI = magnetic resonance imaging, NPC = nasopharyngeal carcinoma.

Keywords: chemoradiotherapy, dynamic contrast enhancement, intravoxel incoherent motion, magnetic resonance imaging, nasopharyngeal carcinoma, sensitivity and specificity, tumor response

---

1. Introduction

Nasopharyngeal carcinoma (NPC) is a common malignancy in Southern China and Southeast Asia, with an incidence of 15/100,000 to 24/100,000.[1] Presently, induction chemotherapy (IC) combined with radiation therapy is the primary treatment for advanced NPC,[2] but not all patients respond well to chemoradiotherapy (CRT). Local residual or relapse is the main reason for treatment failure of NPC patients.[3] Identifying poor-responder before treatment or early in the course of treatment would allow treatment regimens to be modified in a timely manner. Therefore, it would be advantageous to find new imaging markers that could early predict therapeutic response either before treatment or in the early period of therapy.

Multiple imaging modalities can be used to evaluate the early response to treatment for tumors. ^{18}F-Fluoro-deoxy-glucose positron emission tomography (^{18}F-FDG-PET) has been applied in assessing the treatment response for NPC[4] and other tumors such as head and neck squamous cell carcinoma (HNSCC),[5,6] rectal cancer,[7] and breast cancer.[8] However, the complex anatomy of nasopharynx, low spatial resolution, and treatment-

induced inflammation may decrease the accuracy of ^{18}F-FDG-PET.[3] Moreover, its high cost and radiation side effects make it more suboptimal in evaluating treatment response for tumors. In recent years, dynamic contrast-enhanced magnetic resonance imaging MRI (DCE-MRI) and diffusion- weighted imaging (DWI) have been used in the evaluation of treatment response for many types of tumors. DWI, with the ability to measure the motion of water molecules by calculating the apparent diffusion coefficient (ADC) value, allows for a quantitative analysis of tissue microstructure. Previous studies have demonstrated the efficacy of the ADC value for predicting or early detecting the early response to IC or CRT for NPC patients, although variable results have been reported.[2,9–10] Intravoxel incoherent motion diffusion-weighted imaging (IVIM-DWI), a new DWI technique based on the bi-exponential model developed by Le Bihan,[11] allows for the contemporary acquisition of diffusion and perfusion information in tissues. IVIM-DWI is believed to be more accurate than conventional DWI that is based on the mono-exponential decay model and completely overlooks the influence of microcirculation perfusion on diffusion signal intensity. In addition, a recent study by Xiao et al[12] reported that IVIM-DWI can potentially predict the early treatment response to neo-adjuvant chemotherapy in NPC patients. Another recent preliminary study[13] also demonstrated the efficacy of IVIM-DWI in predicting the early effects of IC and CRT in advanced NPC.

It is well known that angiogenesis and blood perfusion are essential factors for tumor progression and are closely associated with curative effect of malignant tumors. DCE-MRI, another MRI perfusion technique, can characterize the vascularity and perfusion of tissue. It has been proven that early changes in DCE-MRI parametric values after chemotherapy can predict the response to CRT in patients with NPC.[14] However, the above-mentioned studies only investigated the early therapeutic response, namely they only evaluated the status of primary tumors at the end of CRT. In fact, early predicting a longer term treatment response could help in defining individualized regimens, earlier modifying treatment regimens, and consequently decreasing medical costs. Therefore, a longer follow-up period is required to predict the longer term effect of CRT in NPC patients. The utility of IVIM-DWI and DCE-MRI in predicting the short-term (i.e., several months after the end of CRT) response to CRT in NPC patients is still unknown and it may be different from that in predicting the early response. Therefore, the aim of this study was to investigate the utility of IVIM-DWI and DCE-MRI in predicting the early and short-term responses to CRT in patients with NPC.

2. Materials and methods

2.1. Patient selection, treatment procedure, and response assessment

This prospective single-center study was approved by the Medical Ethics Committee of our institution (approval number: 2014-8), and informed consent was obtained from all patients. Fifty-one consecutive patients were initially recruited. Patients were included into the study if they had a diagnosis and pathological confirmation of NPC; were >18 years of age; were scheduled for IC and CRT; and had a Karnofsky score ≥80. Patients were excluded if they: had received prior antitumor treatment for NPC; did not sign the informed consent form; or had contraindications for MRI, IC, or CRT.

Each patient's tumor node metastasis (TNM) stage was determined by 2 radiologists after discussion and consensus and was based on the 7th edition of International Union Against Cancer/American Joint Committee on Cancer (UICC/AJCC) staging system,[15] an MRI examination of the head and neck, a computed tomography (CT) scan of the chest, and an MRI examination and/or nuclear medicine examination of the other parts of the body. All patients received a 2-cycle IC (21 days per cycle) that consisted of 135 to 175 mg/m^2 paclitaxel on day 1 accompanied by 80 mg/m^2 nedaplatin on days 1, 2, and 3. After IC, all patients received radiotherapy with a total dose of 70 to 76 Gy and 30 to 33 times to completion.

Based on whether locoregional lesion was identified on MRI and pharyngorhinoscopy, the patients were divided into the residual and nonresidual groups at the end of CRT, and into the good-responder and poor-responder groups 6 months after the end of CRT.

2.2. Conventional MRI protocol

The MRI examinations were performed on a 1.5-Tesla MRI scanner (Optima MR360, GE Healthcare, Milwaukee, WI) at baseline, after the first cycle of IC, at the end of CRT, and 6 months after the end of CRT. The imaging protocols included axial T1-weighted spin-echo images (repetition time [TR]/echo time [TE] 580/7.8 ms, slice number 36, slice thickness 5 mm, slice space 1 mm, number of excitations [NEX] 2, scan time 1 minute 53 seconds) and axial T2-weighted spin-echo images with fat suppression (TR/TE 6289 ms/85 ms, slice number 36, slice thickness 5 mm, slice space 1 mm, NEX 2, scan time 1 minute 35 seconds).

2.3. IVIM-DWI protocol

IVIM-DWI was performed on all patients at baseline and after the first cycle of IC. Ten *b* values (0, 50, 80, 100, 150, 200, 400, 600, 800, and 1000 s/mm^2) were applied with a single-shot diffusion-weighted spin-echo echo-planar (ssSE-DW-EPI) sequence. The lookup table of gradient directions was modified to allow multiple *b* value measurements in 1 series. Parallel imaging was used with an acceleration factor of 2. A local shim box covering the nasopharyngeal region was used to minimize susceptibility artifacts. A total of 12 axial slices covering the nasopharynx were obtained with a 22 cm field of view (FOV), 5 mm slice thickness, 1 mm slice space, TR/TE 4225 ms /106 ms, 128 × 130 matrix, NEX 4, and scan time 2 minutes 55 seconds.

2.4. DCE-MRI protocol

After the conventional MRI and IVIM-DWI, multiphase T1-weighted DCE-MRI images plus pre-contrast T1 mapping were obtained using a spoiled gradient echo sequence (liver acquisition with volume acceleration, LAVA) in the axial plane. Scan parameters were as follows: T1 mapping: flip angle 6°, TR/ TE 3 ms/1.3 ms, FOV 38 cm, slice thickness 5 mm, slice space 1 mm, slice number 16; and contrast-enhanced multiphase T1-weighted MRI acquisition: flip angle 15°, TR/TE 3 ms/1.3 ms, FOV 38 cm, slice thickness 5 mm, slice space 1 mm, slice number 16. Multiphase datasets were acquired every 6 seconds for 56 repetitions. The total scan time for DCE-MRI was 5 minutes 42 seconds. Intravenous contrast agent injection was trigged 15 seconds after the initial multiphase MRI data acquisition by using a power injector. Gadodiamide (Omniscan, GE Healthcare, NJ)

was administered as contrast agent at a dose of 0.1 mmol/kg of body weight and a ratio of 3.5 mL/s, followed by a bolus injection of 20 mL normal saline.

2.5. IVIM-DWI and DCE-MRI analyses

All MRI data were transferred to an Advantage Workstation with Functool software (version AW 4.6, GE Medical Systems, Milwaukee, WI) for post-processing. The DCE-MRI analysis was performed using Cinetool, a software kit for quantitative perfusion evaluation included in the Functool package. DCE-MRI parametric (K^{trans} [the volume transfer constant of the contrast agent], K_{ep} [rate constant], and V_e [the extravascular extracellular volume fraction of the tissue]) maps were calculated automatically on the base of the Tofts–Kermode model.[16,17] According to the Levenberg–Marquardt algorithm,[18] the IVIM data was fitted to a bio-exponential plot on a pixel-by-pixel basis to obtain the IVIM-DWI parametric (D [pure diffusion coefficient], D^* [pseudo-diffusion coefficient], f [perfusion fraction], and ADC).

The IVIM-DWI and DCE-MRI parametric values for each tumor were independently and double-blindly measured by 2 radiologists (H.J. and W.L.) who each had 10 years of experience in head and neck radiology in our department. They were blinded to the results of the response to CRT for all patients. First, the axial image section showing the primary tumor at its widest cross-section was determined using T2-weighted and contrast-enhanced T1-weighted images as references. Three regions of interest (ROIs) were then manually drawn on axial T2-weighted images by each observer for each tumor at its widest section plus adjacent up and down sections to cover as much of the nasopharyngeal tumor as possible while avoiding the areas of necrosis, air, large vessels, and adjacent anatomical structures (i.e., fat, muscle, and bone), and then subsequently co-registered to IVIM DWI images for further analysis. Each metric value was acquired by each observer and 2 initial data points were generated, each of which was the average of the values obtained from the 3 ROIs by 1 observer. The eventual metric value for each tumor was the mean value of the 2 initial data points. The average size of the ROIs was 478.22 ± 356.17 mm^2.

2.6. Statistical analysis

The IVIM-DWI and DCE-MRI parametric values for each group were expressed as the mean ± standard deviation. The percentage changes of the IVIM-DWI and DCE-MRI parametric values were calculated by dividing the mathematical difference of the corresponding parametric values at pretreatment and after the first cycle of IC by the pretreatment parameter value. For example, $\Delta\% K^{trans} = (post-K^{trans} - pre-K^{trans}) / pre-K^{trans}$.

The Pearson χ^2 test or Fisher exact test was used for comparing the clinical characteristics. The Mann–Whitney U test was performed to compare the IVIM-DWI and DCE-MRI parametric values at baseline (pre-ADC, pre-D, pre-D^*, pre-f, pre-K^{trans}, pre-K_{ep}, and pre-V_e), after the first cycle of IC (post-ADC, post-D, post-D^*, post-f, post-K^{trans}, post-K_{ep}, and post-V_e) and the percentage changes of the parametric values ($\Delta\%$ADC, $\Delta\%D$, $\Delta\%D^*$, $\Delta\%f$, $\Delta\%K^{trans}$, $\Delta\%K_{ep}$, and $\Delta\%V_e$) between the nonresidual and residual groups and between the good-responder and poor-responder groups. Receiver operating characteristic (ROC) curve analysis was applied to determine the discrimination power of the IVIM-DWI and DCE-MRI parameters for predicting the curative response. Factors affecting the early and short-term curative effects were further assessed using multivariate logistic regression. Additionally, leave-one-out cross validation was applied to test the finding. All data were analyzed using SPSS version 19.0 (SPSS Inc., Chicago, IL) or MedCalc version 15.0 software (MedCalc Software bvba, Ostend, Belgium). Differences were considered significant if the P value was <0.05.

2.7. Data deposition

All data of the present study will be deposited at http://www.chictr.org.cn/index.aspx (Registration number: ChiCTR-DCD-15006674).

3. Results

From April 2014 to May 2015, 51 consecutive patients were initially recruited. Of these patients, 8 were eliminated from this study because of serious image distortion (n=3), dental artifacts (n=2), withdrawal by patients (n=1), or receiving other antitumor treatment after the end of CRT (n=2). The remaining 43 patients (35 men and 8 women; mean age 48 ± 11.41 years) were finally enrolled in the present study. The pathological type of the 43 patients included 29 undifferentiated and 14 differentiated nonkeratinizing carcinomas. The TNM stage distribution was as follows: T1, n=0 (0%); T2, n=2 (4.7%); T3, n=24 (55.8%); T4, n=17 (39.5%); N0, n=3 (7.0%); N1, n=9 (20.9%); N2, n=24 (55.8%); N3, n=7 (16.3%); M0, n=43 (100.0%); and M1, n=0 (0%). The clinical characteristics of the recruited patients are listed in Table 1.

At the end of CRT, 15 patients had residual lesion in the nasopharynx and 28 did not. Six months after the end of CRT, 35 patients were classified into the good-responder group and 8 into the poor-responder group. Representative pathology and MRI images of patients with different response to CRT are shown in Figs. 1 and 2.

The differences in the clinical characteristics, IVIM-DWI and DCE-MRI parametric values between the residual and nonresidual groups and between the good-responder and poor-responder groups are shown in Tables 2–4, respectively. For the pre-ADC, pre-D, and $\Delta\%D$ values, significant differences were found between the residual and nonresidual groups. The nonresidual group had lower pre-ADC, lower pre-D, and higher $\Delta\%D$ values than did the residual group. There were significant differences between the good-responder and poor-responder groups in T stage, pre-ADC, pre-D, and post-D values. However, none of the perfusion-related parametric values derived from DCE-MRI and IVIM-DWI showed significant differences between either the residual and nonresidual groups or the good-responder and poor-responder groups.

The diagnostic efficacy of pre-ADC, pre-D, and $\Delta\%D$ in distinguishing the nonresidual from residual groups is shown in Fig. 3 and Table 5. Figure 3 and Table 6 show the power of pre-ADC, pre-D, and post-D in discriminating the good-responder from poor-responder group. Logistic regression analysis (forward stepwise, LR; probability for stepwise entry, 0.05; removal, 0.1) indicated that pre-D ($P=0.006$) was the only independent variable for predicting the early response to CRT, whereas both pre-D ($P=0.008$) and T stage ($P=0.002$) were independently predictive factors for short-term outcome in NPC. Base on leave-one-out cross validation, the percentage of correct prediction for pre-D in predicting the early response to CRT was 74.4%, and for pre-D plus T stage in predicting the short-term response is 86.0%.

Table 1

Summary of the clinical characteristics of the 43 patients with NPC.

Patient no.	Sex	Age, y	TNM stages
1	M	64	T4N0M0
2	F	38	T3N2M0
3	M	38	T3N3M0
4	F	49	T3N2M0
5	F	47	T3N2M0
6	M	31	T4N2M0
7	M	60	T3N2M0
8	M	49	T4N0M0
9	M	68	T4N2M0
10	M	32	T4N1M0
11	M	37	T3N2M0
12	M	47	T3N1M0
13	M	38	T4N2M0
14	M	41	T3N3M0
15	M	61	T4N2M0
16	F	27	T2N2M0
17	M	55	T3N1M0
18	M	48	T3N2M0
19	M	45	T4N1M0
20	F	64	T4N2M0
21	F	58	T3N0M0
22	M	47	T3N2M0
23	M	55	T4N2M0
24	M	26	T3N2M0
25	M	37	T4N2M0
26	M	63	T3N2M0
27	M	36	T3N1M0
28	M	26	T3N1M0
29	M	39	T3N3M0
30	M	45	T3N2M0
31	M	58	T3N1M0
32	M	50	T4N2M0
33	M	54	T4N2M0
34	M	49	T4N3M0
35	F	55	T3N2M0
36	M	66	T4N2M0
37	M	63	T4N3M0
38	M	51	T4N3M0
39	F	61	T2N2M0
40	M	47	T3N1M0
41	M	51	T3N3M0
42	M	58	T3N2M0
43	M	45	T3N1M0

NPC = nasopharyngeal carcinoma, TNM = tumor node metastasis.

4. Discussion

This study focused on the value of MRI in predicting the response to CRT in patients with NPC. To the best of our knowledge, this may be the first report to compare the utility of DCE-MRI and IVIM-DWI for predicting the early and short-term responses with CRT for NPC. Our preliminary data showed that IVIM-DWI rather than DCE-MRI could predict the early and short-term curative responses to CRT in NPC patients. In addition, the diffusion-related parameters (pre-ADC, pre-D, and $\Delta\%D$) are superior to the perfusion-related IVIM-DWI parameters (f and D^*) in predicting the response to CRT for NPC.

DCE-MRI can quantify microcirculation perfusion and capillary permeability in tissues.[19] DCE-MRI provides 2 perfusion parameters including K^{trans} and K_{ep}. The former reflects a combination of tumor blood, microvascular permeability, and capillary surface area, whereas the latter only represents vessel permeability. In this study, similar pre-K^{trans} and pre-K_{ep} values were found between the residual and nonresidual groups and between the good-responder and poor-responder groups, indicating that pretreatment perfusion parameters may have little efficacy in the prediction of early and short-term therapeutic responses to CRT for NPC patients. This result is in contrast to several previous studies in which tumors with higher pre-K^{trans} value showed a better response to CRT and led to longer survival in patients with HNSCC,[20] cervical carcinoma,[21–23] breast cancer,[24] non-small cell lung cancer,[25] or glioma.[26] The failure of baseline perfusion parameters derived from DCE-MRI in predicting early and short-term therapeutic response might be because of a widely accepted theory that poor blood supply in tumor will lead to intratumor chronic hypoxia, and thereby promote the transfer of tumor cells into subtypes with more resistance to chemotherapy and radiation, which results in a poor prognosis. Therefore, high intratumor blood flow and blood volume are associated with low level of hypoxia, which will lead to a better therapeutic effect.[27] However, from another point of view, tumors with higher perfusion are always associated with higher degree of malignancy that often has a negative impact on curative effect.[28] In addition, the angiogenesis of neoplastic tissue differs significantly from that of normal tissue. For example, there are more shunts and tortuous pattern of vessels in tumors with high perfusion, which can reduce the delivery of chemotherapeutic agents into tissues and correspondingly leads to treatment resistance.[29,30] The phenomenon that the above-mentioned factors counteract each other might explain the failure of the pre-K^{trans} and pre-K_{ep} values in predicting the early and short-term responses to CRT in NPC. Moreover, the efficacy of DCE-MRI in predicting the therapeutic response may depend on the type of cancers, therapy methods, and imaging protocols. Besides the pre-K^{trans} and pre-K_{ep}, there were also no significant differences in the percentage changes of K^{trans} and K_{ep} values (i.e., $\Delta\%K^{trans}$ and $\Delta\%K_{ep}$) between either the nonresidual and residual groups or the good-responder and poor-responder groups, indicating that the early perfusion variation in tumors induced by IC may have little benefit for predicting both the early and short-term responses to CRT for NPC.

In addition to K^{trans} and K_{ep}, DCE-MRI provides another perfusion parameter, V_e. In the present study, the V_e-related parametric values (pre-V_e, post-V_e, and $\Delta\%V_e$) were not obviously different between either the residual and nonresidual groups or the good-responder and poor-responder groups. Several previous studies on a variety of tumors[31,32] also failed to show significant differences in the V_e value between the responders and non-responders. However, one study by Guo et al[33] demonstrated that V_e may serve as a prognostic biomarker for chemotherapy in osteosarcoma patients. These conflicting results suggest that the efficacy of the V_e value in predicting therapeutic response may depend on the type of tumor. In addition, V_e is believed to represent the volume of the extravascular extracellular space (EES). Water molecule diffusion has a direct correlation with EES, and therefore V_e may be related to water diffusion. The present study demonstrated that D, rather than V_e, is helpful in discriminating between the residual and nonresidual groups and between the good-responder and poor-responder groups. Previous studies also confirmed the utility of D in predicting the early treatment response for NPC.[12,13] Considering that D is simultaneously influenced by the intracellular space, extracellular space and membrane integrity whereas V_e only reflects the EES, we speculate that the change in EES might not be enough to predict the therapeutic response in NPC.
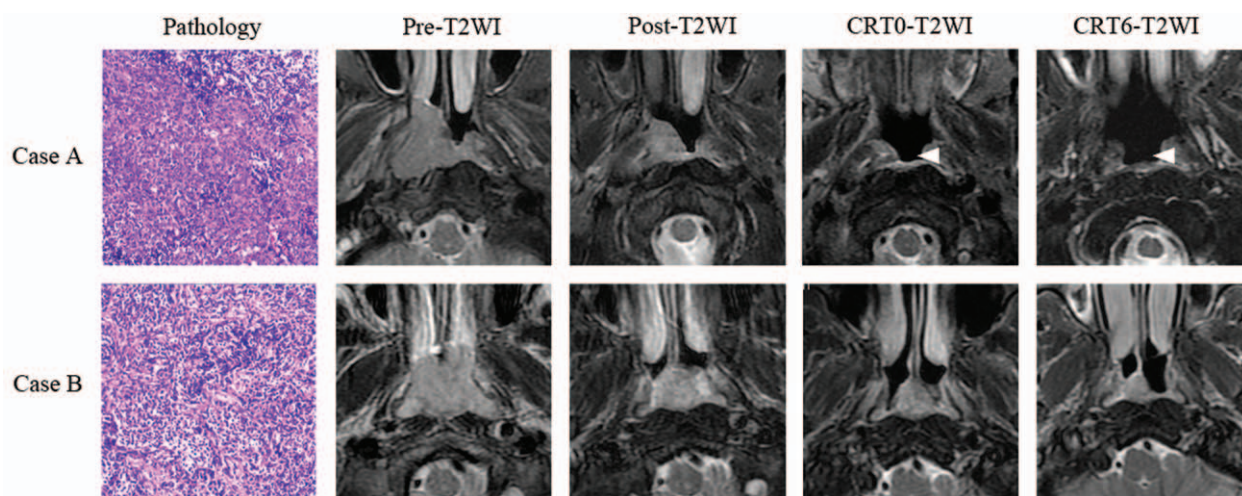
Figure 1. Representative pretreatment pathology and MRI images at 4 different time points from patients with different treatment responses. The upper row shows images from a patient (case A,T3N3M0) in both the nonresidual and good-responder groups, whereas the lower row shows images from a patient (case B, T3N2M0) in both the residual and poor-responder groups. For case A, the primary NPC lesion shrink after 1 cycle of chemotherapy, disappeared (white arrow head) at the end of CRT, and was found without residual or relapse (white arrow head) 6 months after the end of CRT. For case B, the nasopharyngeal tumor shrink after 1 cycle of chemotherapy, but demonstrated residual (white arrow) both at the end of CRT and 6 months after the end of CRT. Pathological sections (hematoxylin-eosin staining, original magnification × 10) demonstrate that the nasopharyngeal carcinoma cell from case A are denser than those from case B, which is consistent with their pretreatment D values shown in Figure 3. CRT = chemoradiotherapy, CRT0 = at the end of CRT, CRT6 = 6 months after the end of CRT, T2WI = T2-weighted imaging.

Based on bi-exponential DWI model, IVIM-DWI can provide 4 parameters (ADC, D, D^*, and f) and concurrently extract diffusion and perfusion information in tissues. In recent years, IVIM-DWI has been used to predict and assess the treatment response in patients with NPC,[12,13] HNSCC,[34] bone metastases,[35] or liver tumors.[36] Therefore, IVIM-DWI is validated as an useful approach for predicting the curative response for many tumors.

Based on the IVIM theory, D corresponds to pure diffusion and is one of the diffusion-related parameters.[18] Depended largely on the ratio of the intracellular and extracellular space in tissues,[37,38] D is generally believed to be inversely correlated with cellularity and positively correlated with necrosis and cystic change in tissues.[12,13] In this study, there were significant differences in the pre-D value between the residual and nonresidual groups and between the good-responder and poor-responder groups, namely both the nonresidual and good-responder groups exhibited lower pre-D value. This implies that tumors with low pretreatment diffusion value, which indicates high cellularity and low extracellular space, will respond better to CRT than will tumors with high diffusion value that indicates low cellularity and much necrosis and cystic change. This result was confirmed by 2 early studies[12,13] in which NPC patients who responded favorably to CRT had significantly lower baseline D value than did those with partial response (PR) and nonresponders. Therefore, these results indicate the feasibility of the pre-D value in predicting the early and short-term responses to CRT for patients with NPC. Furthermore, in the present study, logistic regression analysis indicated that pre-D is an independent prognostic factor for the early and short-term responses to CRT in NPC.

Although an evident increase in the D value (i.e., $\Delta\%D$) was found in all NPC groups in this study, which suggests that effective treatment causes tumor cell death and enlarged extracellular space because of necrosis or apoptosis,[39] there was obvious difference in $\Delta\%D$ only between the nonresidual and residual groups, rather than between the good-responder and poor-responder groups. This finding indicated that greater $\Delta\%D$ after 1 cycle of IC may be predictive of better early response to CRT for patients with NPC, whereas it may be unhelpful in predicting the short-term response to CRT.

ADC, which is a combination of D and D^*, reflects the total diffusion in tissues and primarily depends on D when the b value is $>200\,\text{s/mm}^2$. Therefore, to some extent, ADC is mainly a diffusion-related parameter rather than a perfusion-related parameter at high b values ($>200\,\text{s/mm}^2$). Similar to pre-D, a significantly lower pre-ADC value was found in both the nonresidual and good-responder groups compared with both the residual and poor-responder groups in the present study. Additionally, $\Delta\%D$ exhibited obvious difference between the residual and nonresidual groups, whereas there was no significant difference in $\Delta\%$ADC between either the nonresidual and residual groups or the good-responder and poor-responder groups. In separating the nonresidual from the residual groups, pre-D showed the highest area under the curve (AUC), moderate sensitivity and highest specificity, compared with pre-ADC and $\Delta\%D$. Compared with pre-ADC and post-D, pre-D had the highest AUC and specificity in the discrimination between the good-responder and poor-responder groups, according to ROC analysis. Moreover, logistic regression analysis indicated that pre-D, rather than pre-ADC, was the independent variable for predicting both the early and short-term outcome in NPC. Thus, the above-mentioned findings suggest that D is superior to ADC in predicting the early and short-term responses to CRT in NPC patients. Considering that D is a pure diffusion parameter whereas ADC is a hybrid parameter related to both diffusion and perfusion, these findings may indicate that the perfusion negatively influences the efficacy of ADC in predicting the treatment response to CRT for patients with NPC. Therefore, pure diffusion may be an important microenvironment feature related to curative effect in NPC.

According to the IVIM theory, both D^* and f are perfusion-related parameters. In this study, all parameters related to D^*
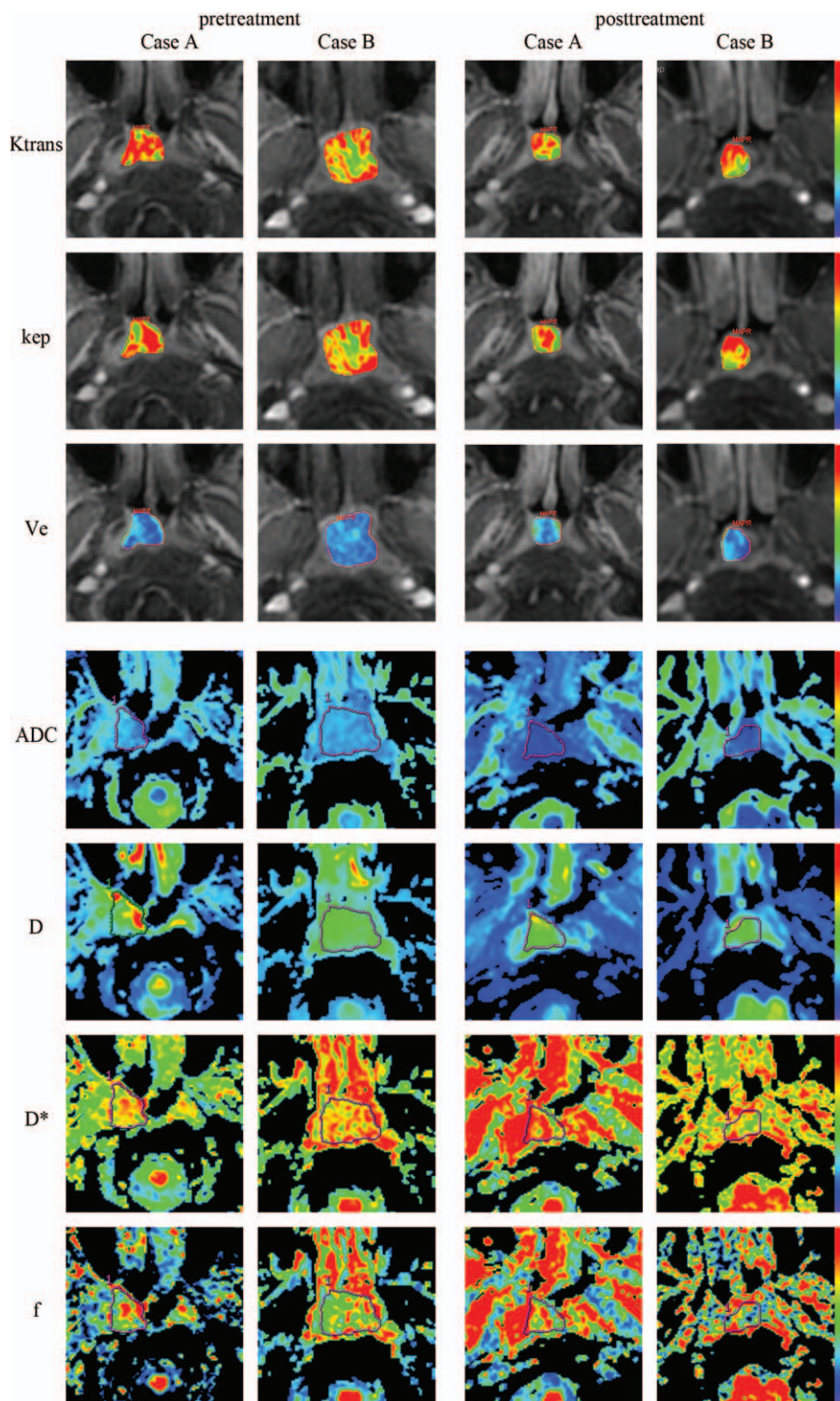
Figure 2. Representative IVIM-DWI and DCE-MRI images before and after the first cycle of induction chemotherapy from 2 patients (case A and case B showed in Figure 2) with different treatment responses. For case A, the K^{trans}, K_{ep}, V_e, ADC, D, D*, and f values at pretreatment are 0.341 min^{-1}, 1.52 min^{-1}, 0.223, 0.766×10^{-3} mm^2/s, 0.587×10^{-3} mm^2/s, 18.000×10^{-3} mm^2/s, and 0.172, respectively, and those values at posttreatment are 0.473 min^{-1}, 1.430 min^{-1}, 0.395, 1.162×10^{-3} mm^2/s, 0.693×10^{-3}mm^2/s, 12.990×10^{-3} mm^2/s, and 0.306 respectively. For case B, the K^{trans}, K_{ep}, V_e, ADC, D, D*, and f values at pretreatment are 0.306 min^{-1}, 1.25 min^{-1}, 0.244, 0.996×10^{-3} mm^2/s, 0.751×10^{-3}mm^2/s, 15.100×10^{-3} mm^2/s, and 0.187,respectively, and those values at posttreatment are 0.574 min^{-1}, 1.530 min^{-1}, 0.378, 1.480×10^{-3} mm^2/s, 0.889×10^{-3}mm^2/s, 9.960×10^{-3} mm^2/s, and 0.542, respectively. The vertical color bar on the right side of parameter maps represents the relative size of MRI parametric value of the pixels in parametric maps. The warmer the color is, the higher the parametric value is. ADC=apparent diffusion coefficient, D*=pseudo- diffusion coefficient, D=pure diffusion coefficient, DCE-MRI=dynamic contrast-enhanced magnetic resonance imaging, f=perfusion fraction, IVIM-DWI=intravoxel incoherent motion diffusion-weighted imaging, K_{ep}=rate constant, K^{trans}=volume transfer constant of the contrast agent, V_e=volume fraction of extravascular extracellular space.

Table 2

Differences in the clinical characteristics between the residual and nonresidual groups and between the poor-responders and good-responders groups.

Clinical characteristics	No. of patients with residual	No. of patients without residual	χ^2	P value	No. of poor responders	No. of good responders	χ^2	P value
Sex			0.057	0.811			0.000	0.991
Male	12	23			7	28		
Female	3	5			1	7		
Pathology			0.177	0.674			2.512	0.113
Undifferentiated	9	20			3	26		
Differentiated	6	8			5	9		
T stage			6.305	0.098			13.756	0.003[*]
T1	0	2			0	2		
T2	5	9			1	13		
T3	2	11			0	13		
T4	8	6			7	7		

[*] $P<0.05$.

(i.e., pre-D^*, post-D^*, and $\Delta\%D^*$) and f (i.e., pre-f, post-f, and $\Delta\%f$) did not show significant differences between either the residual and nonresidual groups or the good-responder and poor-responder groups. These results were consistent with the above-mentioned classical perfusion parameters obtained from DCE-MRI in this study, indicating that the perfusion-related parameters during the course of CRT correlated poorly with the early and short-term curative responses in NPC patients. However, a study by Xiao et al[12] showed that the early changes in the D^* value can effectively differentiate the responders from the nonresponders after neoadjuvant chemotherapy for NPC patients. The differences in therapeutic methods and time points

selected for predicting therapeutic response between our and Xiao et al's[12] studies might account for the above-mentioned conflicting results. In addition, it has been widely reported that the measurement of D^* value is usually associated with much poor reproducibility compared with that of f and D.[25–28] Furthermore, the measurement of the f value was found to be greatly dependent on the TE and the T2 relaxation time.[40,41] Finally, the number of low b values used in IVIM-DWI may also influence the measurement accuracy of perfusion-related parameters. Therefore, technical factors may affect the efficacy of perfusion parameters in predicting therapeutic effect.

Table 3

Differences in the IVIM-DWI and DCE-MRI parametric values between the residual and nonresidual groups.

Parameters	Residual (n=15)	Nonresidual (n=28)	P value
Pre-ADC ($\times 10^{-3}$ mm^2/s)	1.063±0.227	0.930±0.226	0.027[*]
Post-ADC ($\times 10^{-3}$ mm^2/s)	1.449±0.339	1.361±0.371	0.372
$\Delta\%$ADC (%)	38.024±27.168	49.631±39.575	0.541
Pre-D ($\times 10^{-3}$ mm^2/s)	0.838±0.188	0.662±0.115	0.001[†]
Post-D ($\times 10^{-3}$ mm^2/s)	1.089±0.345	0.967±0.289	0.251
$\Delta\%D$ (%)	23.554±30.821	51.593±54.655	0.025[*]
Pre-D^* ($\times 10^{-3}$ mm^2/s)	19.114±16.761	18.758±13.590	0.575
Post-D^* ($\times 10^{-3}$ mm^2/s)	13.401±5.640	10.715±6.777	0.079
$\Delta\%D^*$ (%)	−12.148±82.123	−26.465±56.966	0.108
Pre-f	0.274±0.125	0.257±0.103	0.750
Post-f	0.309±0.095	0.352±0.108	0.231
$\Delta\%f$ (%)	30.291±58.633	52.514±60.063	0.194
Pre-K^{trans}, min^{-1}	0.451±0.195	0.397±0.146	0.379
Post-K^{trans}, min^{-1}	0.534±0.301	0.517±0.248	0.838
$\Delta\%K^{trans}$ (%)	26.227±68.500	41.129±76.730	0.610
Pre-K_{ep}, min^{-1}	0.865±0.535	0.662±0.435	0.173
Post-K_{ep}, min^{-1}	0.814±0.572	0.706±0.412	0.628
$\Delta\%K_{ep}$ (%)	−2.224±74.624	27.272±84.914	0.221
Pre-V_e	0.668±0.367	0.860±0.533	0.252
Post-V_e	0.930±0.675	0.944±0.519	0.610
$\Delta\%V_e$ (%)	46.762±58.378	21.435±40.800	0.212

ADC = apparent diffusion coefficient, D^* = pseudo-diffusion coefficient, D = pure diffusion coefficient, DCE-MRI = dynamic contrast-enhanced magnetic resonance imaging, f = perfusion fraction, IVIM-DWI = intravoxel incoherent motion diffusion-weighted imaging, K_{ep} = rate constant, K^{trans} = volume transfer constant of the contrast agent, V_e = the extravascular extracellular volume fraction.
[*] $P<0.05$.
[†] $P<0.01$.

Table 4

Differences in the IVIM-DWI and DCE-MRI parametric values between the good-responder and poor-responder groups.

Parameters	Poor-responder (n=8)	Good-responder (n=35)	P value
Pre-ADC ($\times 10^{-3}$ mm^2/s)	1.113±0.256	0.946±0.219	0.034*
Post-ADC ($\times 10^{-3}$ mm^2/s)	1.549±0.372	1.356±0.351	0.160
$\Delta\%$ADC (%)	41.863±33.198	46.433±36.816	0.851
Pre-D ($\times 10^{-3}$ mm^2/s)	0.878±0.174	0.688±0.144	0.002[†]
Post-D ($\times 10^{-3}$ mm^2/s)	1.270±0.332	0.950±0.277	0.013*
$\Delta\%D$ (%)	37.125±33.879	42.883±52.407	0.876
Pre-D^* ($\times 10^{-3}$ mm^2/s)	21.263±21.920	17.966±12.562	0.662
Post-D^* ($\times 10^{-3}$ mm^2/s)	12.962±6.576	11.352±6.499	0.585
$\Delta\%D^*$ (%)	5.392±81.143	-17.198±65.797	0.417
Pre-f	0.241±0.073	0.268±0.117	0.564
Post-f	0.285±0.087	0.349±0.106	0.142
$\Delta\%f$ (%)	23.427±36.282	49.638±63.401	0.275
Pre-K^{trans}, min^{-1}	0.490±0.225	0.399±0.146	0.261
Post-K^{trans}, min^{-1}	0.551±0.195	0.517±0.279	0.596
$\Delta\%K^{trans}$ (%)	25.218±59.915	38.380±76.805	0.779
Pre-K_{ep}, min^{-1}	0.815±0.423	0.714±0.491	0.435
Post-K_{ep}, min^{-1}	0.713±0.347	0.750±0.497	0.901
$\Delta\%K_{ep}$ (%)	10.737±82.971	20.317±82.245	0.512
Pre-V_e	0.661±0.365	0.823±0.509	0.382
Post-V_e	0.881±0.358	0.952±0.612	0.827
$\Delta\%V_e$ (%)	50.872±58.989	25.561±45.501	0.333

ADC = apparent diffusion coefficient, D^* = pseudo-diffusion coefficient, D = pure diffusion coefficient, DCE-MRI = dynamic contrast-enhanced magnetic resonance imaging, f = perfusion fraction, IVIM-DWI = intravoxel incoherent motion diffusion-weighted imaging, K_{ep} = rate constant, K^{trans} = volume transfer constant of the contrast agent, V_e = extravascular extracellular volume fraction.
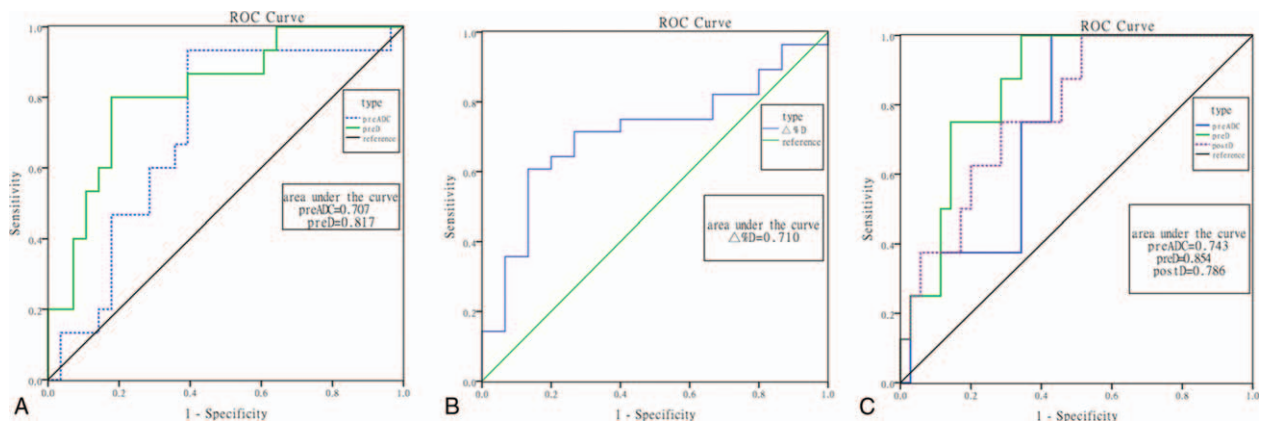[*] $P<0.05$.
[†] $P<0.01$.

Figure 3. The diagnostic accuracy of IVIM-DWI parameters in predicting tumor responses at the end of CRT and 6 months after the end of CRT. Receiver operating characteristic curve (A) shows the diagnostic accuracy of pre-ADC (blue) and pre-D (green) in predicting tumor residue after CRT; curve (B) shows the diagnostic accuracy of $\Delta\%D$ in predicting residue after CRT; curve (C) shows the diagnostic accuracy of pre-ADC (blue), pre-D (green), and post-D (purple) in predicting tumor response 6 months after the end of CRT. ADC = apparent diffusion coefficient, CRT = chemoradiotherapy, D = pure diffusion coefficient, IVIM-DWI = intravoxel incoherent motion diffusion-weighted imaging.

Table 5

Diagnostic efficacy of IVIM-DWI parameters in predicting the residual and nonresidual groups.

Parameters	Cut off Value	Sensitivity (%)	Specificity (%)	AUC (95% CI)
Pre-ADC	0.859×10^{-3} mm^2/s	93.33	60.71	0.707 (0.549–0.836)
Pre-D	0.721×10^{-3} mm^2/s	80.00	82.14	0.817 (0.669–0.918)
$\Delta\%D$	33.89%	86.67	60.71	0.710 (0.551–0.838)

ADC = apparent diffusion coefficient, AUC = area under the curve, CI = confidence interval, D = pure diffusion coefficient, IVIM-DWI = intravoxel incoherent motion diffusion-weighted imaging.

It is well known that both diffusion and perfusion are microenvironment characteristics that could potentially predict the therapeutic effect for many kinds of tumors. Although both IVIM-DWI and DCE-MRI can quantify the perfusion features of tissues, the 2 perfusion-related MRI approaches are based on different theories and mathematical models. The perfusion-related MRI parameters (D^* and f) and DCE-MRI perfusion parameters (K^{trans}, K_{ep}, and V_e) respectively represent different microenvironment characteristics related to perfusion. In the present study, we simultaneously compared the utility of diffusion-related MRI parameters with both perfusion-related IVIM parameters and DCE-MRI perfusion parameters in predicting the early and short-term responses to CRT in NPC. Our results revealed that diffusion-related MRI parameters are more valuable than perfusion-related MRI parameters derived from different MRI perfusion techniques. Considering that a previous study[13] demonstrated that diffusion-related MRI parameters are more powerful than perfusion-related metrics in predicting the early response to IC and CRT for NPC, our study further confirms that diffusion is more important than perfusion in predicting the response to CRT for NPC.

There are some limitations in this study. Firstly, the study cohort was relatively small, and the patients were not divided into subgroups based on TNM stages. However, tumor stage is significant for the therapeutic response and prognosis. Thus, further studies with larger cohorts are needed to perform an analysis of a subgroup of patients stratified by TNM stages, which may reduce the statistical bias. Secondly, this study mainly focused on the early and short-term responses to CRT rather than the long-term response. A longer follow-up period is required to determine whether IVIM-DWI and DCE-MRI could be used to predict the longer-term effect of CRT for NPC.

In conclusion, this preliminary study investigated the role of IVIM-DWI and DCE-MRI as potential imaging approaches for predicting the therapeutic effect in NPC. Our findings revealed that IVIM-DWI is more valuable than DCE-MRI in predicting the early and short-term responses to CRT for NPC, and furthermore diffusion-related IVIM-DWI parameters are more powerful than perfusion-related parameters derived from both IVIM-DWI and DCE-MRI.

Table 6

Diagnostic efficacy of IVIM-DWI parameters in predicting the good-responder and poor-responder groups.

Parameters	Cut off Value	Sensitivity (%)	Specificity (%)	AUC (95% CI)
Pre-ADC	0.898×10^{-3} mm^2/s	100	57.14	0.743 (0.587–0.864)
Pre-D	0.711×10^{-3} mm^2/s	100	65.71	0.854 (0.712–0.943)
Post-D	0.914×10^{-3} mm^2/s	100	48.57	0.786 (0.634–0.896)

ADC = apparent diffusion coefficient, AUC = area under the curve, CI = confidence interval, D = pure diffusion coefficient, VIM-DWI = intravoxel incoherent motion diffusion-weighted imaging.

References

[1] Hao Peng , Lei Chen , Yuan Zhang , et al. The tumour response to induction chemotherapy has prognostic value for long-term survival outcomes after intensity-modulated radiation therapy in nasopharyngeal carcinoma. Sci Rep 2016;6:24835.

[2] Chen Y, Liu X, Zheng D, et al. Diffusion-weighted magnetic resonance imaging for early response assessment of chemoradiotherapy in patients with nasopharyngeal carcinoma. Magn Reson Imaging 2014;32:630–7.

[3] Shen T, Tang LQ, Luo DH, et al. Different prognostic values of plasma Epstein–Barr virus DNA and maximal standardized uptake value of 18F-FDG PET/CT for nasopharyngeal carcinoma patients with recurrence. PloS One 2015;10:e0122756.

[4] Zhou H, Shen G, Zhang W, et al. 18F-FDG PET/CT for the diagnosis of residual or recurrent nasopharyngeal carcinoma after radiotherapy: a meta-analysis. J Nucl Med 2016;57:342–7.

[5] Castaldi P, Leccisotti L, Bussu F, et al. Role of 18 F-FDG PET-CT in head and neck squamous cell carcinoma. Acta Otorhinolaryngol Ital 2013;33:1–8.

[6] Gavid M, Prevot-Bitot N, Timoschenko A, et al. [18F]-FDG PET-CT prediction of response to induction chemotherapy in head and neck squamous cell carcinoma: preliminary findings. Eur Ann Otorhinolaryngol Head Neck Dis 2015;132:3–7.

[7] Maffione AM, Marzola MC, Capirci C, et al. Value of (18)F-FDG PET for predicting response to neoadjuvant therapy in rectal cancer: systematic review and meta-analysis. AJR Am J Roentgenol 2015;204:1261–8.

[8] Groheux D, Hindié E, Marty M, et al. (18)F-FDG-PET/CT in staging, restaging, and treatment response assessment of male breast cancer. Eur J Radiol 2014;83:1925–33.

[9] Zheng D, Chen Y, Chen Y, et al. Early assessment of induction chemotherapy response of nasopharyngeal carcinoma by pretreatment diffusion-weighted magnetic resonance imaging. J Comput Assist Tomogr 2013;37:673–80.

[10] Hong J, Yao Y, ZhangF Y , et al. Value of magnetic resonance diffusion-weighted imaging for the prediction of radiosensitivity in nasopharyngeal carcinoma. Otolaryngol Head Neck Surg 2013;149:707–13.

[11] Le Bihan D. Intravoxel incoherent motion perfusion MR imaging: a wake-up call. Radiology 2008;249:748–52.

[12] Xiao Y, Pan J, Chen Y, et al. Intravoxel incoherent motion-magnetic resonance imaging as an early predictor of treatment response to neoadjuvant chemotherapy in locoregionally advanced nasopharyngeal carcinoma. Medicine 2015;94:e973.

[13] Yu XP, Hou J, Li FP, et al. Intravoxel incoherent motion magnetic resonance imaging for predicting early response to induction chemotherapy and chemoradiotherapy in patients with nasopharyngeal carcinoma. J Magn Reson Imaging 2016;43:1179–90.

[14] Zheng D, Chen Y, Liu X, et al. Early response to chemoradiotherapy for nasopharyngeal carcinoma treatment: value of dynamic contrast-enhanced 3.0 T MRI. J Magn Reson Imaging 2015;41:1528–40.

[15] Edge SB, Compton CC. The American Joint Committee on Cancer: the 7th edition of the AJCC cancer staging manual and the future of TNM. Ann Surg Oncol 2010;17:1471–4.

[16] Tofts PS, Kermode AG. Measurement of the blood–brain barrier permeability and leakage space using dynamic MR imaging: fundamental concepts. Magn Reson Med 1991;17:357–67.

[17] Tofts PS. Modeling tracer kinetics in dynamic Gd-DTPA MR imaging. J Magn Reson Imaging 1997;7:91–101.

[18] Le Bihan D, Turner R. The capillary network: a link between IVIM and classical perfusion. Magn Reson Med 1992;27:171–8.

[19] Barrett T, Gill AB, Kataoka MY, et al. DCE and DW MRI in monitoring response to androgen deprivation therapy in patients with prostate cancer: a feasibility study. Magn Reson Med 2012;67:778–85.

[20] Chawla S, Kim S, Loevner LA, et al. Prediction of disease-free survival in patients with squamous cell carcinomas of the head and neck using dynamic contrast-enhanced MR imaging. AJNR 2011;32:778–84.

[21] Hawighorst H, Weikel W, Knapstein PG, et al. Angiogenic activity of cervical carcinoma: assessment by functional magnetic resonance imaging-based parameters and a histomorphological approach in correlation with disease outcome. Clin Cancer Res 1998;4:2305–12.

[22] Loncaster JA, Carrington BM, Sykes JR, et al. Prediction of radiotherapy outcome using dynamic contrast-enhanced MRI of carcinoma of the cervix. Int J Radiat Oncol Biol Phys 2002;54:759–67.

[23] Hawighorst H, Knapstein PG, Knopp MV, et al. Uterine cervical carcinoma: comparison of standard and pharmacokinetic analysis of time-intensity curves for assessment of tumor angiogenesis and patient survival. Cancer Res 1998;58:3598–602.

[24] Bone B, Szabo BK, Perbeck LG, et al. Can contrast-enhanced MR imaging predict survival in breast cancer? Acta Radiol 2003;44:373–8.

[25] Ohno Y, Nogami M, Higashino T, et al. Prognostic value of dynamic MR imaging for non-small-cell lung cancer patients after chemoradiotherapy. J Magn Reson Imaging 2005;21:775–83.

[26] Mills SJ, Patankar TA, Haroon HA, et al. Do cerebral blood volume and contrast transfer coefficient predict prognosis in human glioma? AJNR Am J Neuroradiol 2006;27:853–8.

[27] Donaldson SB, Betts G, Bonington SC, et al. Perfusion estimated with rapid dynamic contrast-enhanced magnetic resonance imaging correlates inversely with vascular endothelial growth factor expression and pimonidazole staining in head-and-neck cancer: a pilot study. Int J Radiat Oncol Biol Phys 2011;81:1176–83.

[28] Zahra MA, Tan LT, Priest AN, et al. Semiquantitative and quantitative dynamic contrast-enhanced magnetic resonance imaging measurements predict radiation response in cervix cancer. Int J Radiat Oncol Biol Phys 2009;74:766–73.

[29] Bernstein JM, Homer JJ, West CM. Dynamic contrast-enhanced magnetic resonance imaging biomarkers in head and neck cancer: potential to guide treatment? a systematic review. Oral Oncol 2014;50:963–70.

[30] Beets-Tan RG, Beets GL. MRI for assessing and predicting response to neoadjuvant treatment in rectal cancer. Nat Rev Gastroenterol Hepatol 2014;11:480–8.

[31] Gollub MJ, Gultekin DH, Akin O, et al. Dynamic contrast enhanced-MRI for the detection of pathological complete response to neoadjuvant chemotherapy for locally advanced rectal cancer. Eur Radiol 2012;22:821–31.

[32] Chawla S, Kim S, Dougherty L, et al. Pretreatment diffusion-weighted and dynamic contrast-enhanced MRI for prediction of local treatment response in squamous cell carcinomas of the head and neck. AJR Am J Roentgenol 2013;200:35–43.

[33] Guo J, Reddick WE, Glass JO, et al. Dynamic contrast-enhanced magnetic resonance imaging as a prognostic factor in predicting event-free and overall survival in pediatric patients with osteosarcoma. Cancer 2012;118:3776–85.

[34] Hauser T, Essig M, Jensen A, et al. Characterization and therapy monitoring of head and neck carcinomas using diffusion-imaging-based intravoxel incoherent motion parameters-preliminary results. Neuroradiology 2013;55:527–36.

[35] Gaeta M, Benedetto C, Minutoli F, et al. Use of diffusion-weighted, intravoxel incoherent motion, and dynamic contrast-enhanced MR imaging in the assessment of response to radiotherapy of lytic bone metastases from breast cancer. Acad Radiol 2014;21:1286–93.

[36] Guo Z, Zhang Q, Li X, et al. Intravoxel incoherent motion diffusion weighted mr imaging for monitoring the instantly therapeutic efficacy of radiofrequency ablation in rabbit VX2 tumors without evident links between conventional perfusion weighted images. PLoS One 2015;10:e0127964.

[37] Shim WH, Kim HS, Choi CG, et al. Comparison of apparent diffusion coefficient and intravoxel incoherent motion for differentiating among glioblastoma, metastasis, and lymphoma focusing on diffusion-related parameter. PLoS One 2015;10:e0134761doi: 10.1371/journal.pone.0134761.

[38] Zhang SX, Jia QJ, Zhang ZP, et al. Intravoxel incoherent motion MRI: emerging applications for nasopharyngeal carcinoma at the primary site. Eur Radiol 2014;24:1998–2004.

[39] Kim S, Loevner L, Quon H, et al. Diffusion-weighted magnetic resonance imaging for predicting and detecting early response to chemoradiation therapy of squamous cell carcinomas of the head and neck. Clin Cancer Res 2009;15:986–94.

[40] Sumi M, Van Cauteren M, Sumi T, et al. Salivary gland tumors: use of intravoxel incoherent motion MR imaging for assessment of diffusion and perfusion for the differentiation of benign from malignant tumors. Radiology 2012;263:770–7.

[41] Lemke A, Laun FB, Simon D, et al. An in vivo verification of the intravoxel incoherent motion effect in diffusion-weighted imaging of the abdomen. Magn Reson Med 2010;64:1580–5.